



Original Paper

Mechanical properties of wall soils for predicting damage to the substrate of *Hiten* wall paintings in the Horyu-ji Temple main hall caused by humidity fluctuation: Measurements with mock-up materials

Kazuki Ishikawa,¹  Daisuke Ogura,²  Chiemi Iba,²  Nobumitsu Takatori²  and Soichiro Wakiya³ 

¹Department of Architecture and Urban Design, School of Regional Design, Utsunomiya University, Utsunomiya, Japan; ²Department of Architecture and Architectural Engineering, Graduate School of Engineering, Kyoto University, Kyoto, Japan; ³Conservation Science Section, Nara National Research Institute for Cultural Properties, National Institutes for Cultural Heritage, Nara, Japan

Correspondence

Kazuki Ishikawa, Department of Architecture and Urban Design, School of Regional Design, Utsunomiya University, Building No. 10, Yoto 7-1-2, Utsunomiya-shi, Tochigi, Japan.
Email: ishikawa.kazuki@cc.utsunomiya-u.ac.jp

Funding information

Part of the present work was supported by the Grant-in-Aid for JSPS Fellows of Japan Society for the Promotion of Science (Grant Number 22J15027 and 22KJ1975) and by the JST SPRING of Japan Science and Technology Agency (Grant Number JPMJSP2110).

Received May 8, 2024; Accepted August 15, 2024

doi: 10.1002/2475-8876.70000

Abstract

Safe and efficient conservation of cultural artifacts requires preventing artifacts deterioration and energy-saving environmental control. To achieve this, predicting deterioration caused by environmental conditions is necessary. Predicting the mechanical damage caused by humidity fluctuations necessitates knowledge of the mechanical properties of cultural artifacts materials. Although the mechanical properties of several artifacts have been extensively studied, no investigations have focused on the soils underlying wall paintings. This study aims to clarify some mechanical properties of the upper- and middle-coat soils serving as the substrates for *Hiten* wall paintings at Horyu-ji Temple. Mock-up materials were prepared, and splitting tensile and uniaxial compressive tests were performed. Simultaneously, specimens with various equilibrium humidities were tested to clarify their humidity dependency. The tensile and compressive strengths, Young's modulus, proportional limit, and Poisson's ratio of the upper-coat soil were 0.103–0.239 MPa, 1.16–2.55 MPa, 0.115–0.209 GPa, and 1.10–2.49 MPa, and 0.152, respectively. Moreover, the humidity-induced strains for the upper- and middle-coat soils were measured, and the moisture expansion coefficients were approximately 1240 and 2337 $\mu\text{ST}/\%$, respectively. The results of this study provide vital data for the conservation of the wall paintings and contribute to a deeper understanding of wall soil properties.

Keywords

heritage conservation, humidity, humidity-induced strain, mechanical tests, mud wall

1. Introduction

1.1 Background

For cultural artifacts stored and exhibited in an indoor environment, improper management of environmental factors, such as heat, humidity, light, and air quality, can lead to their deterioration and loss of their value. Among the environmental factors, inadequate temperature and humidity can induce or accelerate various deterioration phenomena.¹ Therefore, temperature and humidity control is crucial for preserving cultural artifacts. However, achieving environmental control while

reducing energy consumption and costs is also required. To satisfy the energy and cost requirements, clarifying allowable temperature and humidity ranges and rates of change for conservation is beneficial. Besides, predicting the impact of environmental temperature and humidity on deterioration is necessary to evaluate the allowable hygrothermal conditions.

Among the deteriorations depending on temperature and humidity conditions, a typical phenomenon caused by humidity fluctuations is mechanical damage to artifacts made of paper, wood, soil, and other hygroscopic materials. Deformation becomes constrained when the moisture conditions within a

material vary or when materials with different moisture expansion properties are bonded together. This can result in stress and potential mechanical damage. In paintings, layers of materials with different moisture expansion properties are often stacked. Each layer constrains its deformation, resulting in compressive and tensile forces between them. In addition, changes in environmental humidity cause moisture conditions to shift toward equilibrium, starting from the surface. This leads to a distribution of moisture conditions throughout the thickness of the painting, causing deformation and stress distribution within a single material depending on moisture conditions gradients.²

Mechanical damage occurs when stress or deformation exceeds the damage thresholds for each material. Predicting mechanical damage necessitates comparing stress and strain with the damage criteria, such as strength or critical strain. Prediction of stress and strain caused by moisture conditions distribution is enabled by applying constitutive relations to which the effects of swelling and shrinking caused by moisture content changes are introduced. In addition, because moisture transfer is coupled with heat transfer, the moisture conditions distribution in a material can be predicted by applying heat and moisture simultaneous transfer model, such as that in existing literature.³ Therefore, understanding constitutive coefficients, the relationship between moisture conditions and strain, and damage criteria, such as strength, in addition to hygrothermal properties, is necessary for constructing damage prediction models for cultural artifacts.

1.2 Previous studies and motivation

Several studies have been conducted to quantify the mechanical properties of cultural artifact materials. For instance, the elastic moduli and moisture expansion coefficients of oiled paint, poplar wood, lime wood, canvas, gesso, and animal glue used in panel and canvas paintings have been measured.^{4–12} Furthermore, damage criteria, such as strength, strain at break or yield, and energy release ratio (a fracture mechanics parameter) of poplar wood, lime wood, oak wood of various ages, oiled paint, animal glue, gesso, and clay substrate of lacquer, have been obtained.^{6,7,11–15} These mechanical properties used for stress, deformation, and damage prediction have thus far been measured in several cultural artifacts, with their humidity dependence clarified in some cases.^{6,9,11} However, previous studies have predominantly focused on panel and canvas paintings and wooden ornaments. Therefore, mechanical properties of many materials in other cultural artifacts remain unexplored.

Some of the authors are involved in the conservation and exhibition project of the wall paintings in the main hall of Horyu-ji Temple. In this project, predicting the mechanical damage to the wall paintings is crucial for determining the appropriate method for environmental control.² Therefore, clarifying the mechanical properties of the materials used for the wall paintings is an urgent issue. Assuming that the wall painting substrates are brittle materials, the maximum principal stress criterion, which predicts damage occurring by comparing the maximum or minimum principal stresses to the tensile or compressive strength, respectively is an effective means of conducting damage prediction of the wall paintings. To apply the criterion, the strengths must be clarified. In addition, the stress–strain relationship in isotropic materials, incorporating the deformation derived from wetting or drying, is expressed as

$$\sigma_{ii} = D_1 \varepsilon_{ii} + D_2 (\varepsilon_{jj} + \varepsilon_{kk}) - D_3 e \Delta h, \quad (1)$$

$$\tau_{ij} = D_4 \gamma_{ij}, \quad (2)$$

$$D_1 = \frac{E(1-\nu)}{(1+\nu)(1-2\nu)}, \quad (3)$$

$$D_2 = \frac{E\nu}{(1+\nu)(1-2\nu)}, \quad (4)$$

$$D_3 = \frac{E(1+\nu)}{(1+\nu)(1-2\nu)}, \quad (5)$$

$$D_4 = \frac{E}{2(1+\nu)}, \quad (6)$$

where σ_{ii} and τ_{ij} are the vertical and shear stresses, respectively, ε_{ii} and γ_{ij} are the vertical and shear strains, respectively, and e is the moisture expansion coefficient which gives the strain relative to the equilibrium RH change Δh . To predict the stresses using Equations (1)–(6), the elastic moduli and moisture expansion coefficient of wall painting substrates must be clarified on the assumption that the materials are isotropic.

Figure 1 shows present *Hiten* wall painting (No. 16), and Figure 2 shows the constituent materials of the wall paintings inferred from previous research on the wall paintings in Horyu-ji Temple.^{16–19} The wall paintings have soil wall substrates composed of various types of wall soil (*Kabe-tsuchi*). The thicknesses of the upper-, middle-, and under-coat soil layers were based on the research of Aoyagi and Hayashi,¹⁹ in which they estimated the dimensions of various parts of the burned wall paintings based on the documents stored at Horyu-ji Temple. Note that the assumption of the materials and composition of *Hiten* wall paintings presented in Figure 2 are based on studies of the burned wall paintings, which were originally the first-story walls in the main hall of Horyu-ji Temple. The main focus of this study is *Hiten* wall paintings, which were not burned, and their materials and compositions have not been clarified. We assumed that the materials and



FIGURE 1 One of *Hiten* wall paintings in the storehouse of the main hall of Horyu-ji Temple photographed by an author (K. Ishikawa) on December 1, 2021

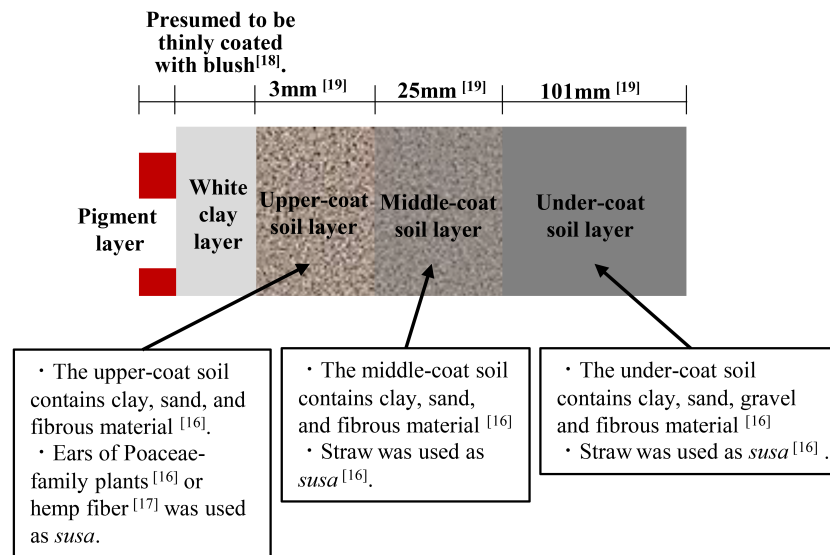


FIGURE 2 Assumption of materials and composition of *Hiten* wall paintings

compositions of *Hiten* wall paintings were identical to those of the burned wall paintings.

Because touching the wall painting is prohibited, and performing mechanical tests on the original wall paintings is difficult, using mock-up wall painting materials is a practical alternative method for estimating mechanical properties. In a previous study, the authors measured the tensile and compressive strengths, Young's modulus, and Poisson's ratio of white clay using a mock-up material.² White clay is a substrate for *Hiten* wall paintings, positioned just beneath the paint layer. To predict the stress and strain leading to damage in the wall paintings, the mechanical properties of further underlying layer material, specifically upper-coat soil (*Hyodo*) and middle-coat soil (*Nakanuri-tsuchi*), are also necessary. Upper- and middle-coat soils are types of wall soils currently used as traditional building materials. Several studies have explored the mechanical properties of wall soils.^{20–29} These studies revealed that the mechanical properties of walls soil vary based on the mixing materials, mixing ratio, and fabrication conditions, such as the length of *mizuawase*, the period after the materials are blended and kept wet. Therefore, obtaining the mechanical properties of wall soils simulating the original materials is necessary for precise damage prediction of the wall paintings. In addition, the mechanical properties of the wall soil are expected to vary significantly with the moisture content of the material because the structure is supported by the bonding of soil particles by the meniscus. Accordingly, experiments have been performed to investigate the relationship between moisture conditions and the mechanical properties of under-coat soil (*Arakabe-tsuchi*).²¹ However, other than the referenced research, knowledge of the relationship between the mechanical properties and moisture conditions of wall soils remains lacking.

1.3 Research purpose

This study aimed to obtain the mechanical properties of upper- and middle-coat soils used as substrates for *Hiten* wall paintings in the main hall of Horyu-ji Temple to contribute to predicting the damage to the wall paintings induced by humidity fluctuations. Mock-up materials for the upper- and middle-coat soils were prepared for measurement. For the mock-up upper-coat

soil, Young's modulus, Poisson's ratio, and compressive strength were obtained through uniaxial compressive test, and the tensile strength was obtained through splitting tensile test. The humidity dependence of these properties was clarified using specimens in equilibrium to different moisture conditions, and the mechanical properties were approximated as functions depending on relative humidity to be utilized in the damage prediction. Moreover, the humidity-induced strains in the mock-up upper- and middle-coat soils were measured, and the relationships between the strain and equilibrium humidity of these materials were identified.

2. Mainly targeting cultural artifacts

In a previous study,² the authors extensively discussed knowledge of *Hiten* wall paintings. The main hall of Horyu-ji Temple is believed to be built in the 7th to early 8th century.¹⁶ The walls under the ceiling of the main hall had 20 *Hiten* wall paintings. The main hall was burned in 1949 during building renovations, severely damaging the building frame and 12 large wall paintings. However, 20 *Hiten* wall paintings remained unscathed because they were removed from the building frame with their substrate soil walls. *Hiten* wall paintings have been designated as important cultural properties by the Japanese government. One of the 20 *Hiten* wall paintings is displayed in the Great Treasure Gallery (*Daihozoin*), and the remaining paintings, along with the burned main hall building frame, are placed in a storehouse. These 19 paintings are usually kept in the storehouse and kept away from public view; however, recent initiatives have begun to make them accessible to the public for a limited period.

As shown in Figure 2, the substrates of the wall paintings comprised soil walls with multiple layers, and white clay was used as the substrate layer for the pigment.¹⁸ The upper-coat soil positions just beneath the white clay, and the middle-coat soil does beneath the upper-coat soil layer. Previous reports^{16,19} identified or estimated the component materials and soil grain sizes of the upper- and middle-coat soils of the burned wall paintings using a water-sieving technique. Based on these reports, the materials, including the grain size of the soils, and composition for the mock-up wall soils were

determined, as described in the subsequent section. The original upper-coat soil was estimated to contain Poaceae-family plant ears and other plant fibers of 8–11 mm in length¹⁶ or hemp fibers.¹⁹ The middle-coat soil contained 13–30 mm straw fibers. However, it should be noted that the report did not describe a separation method for clay and fine sand, although a precipitation method was possibly used. In addition, the report provided the mass ratios of the materials in the upper- and middle-coat soils, but the humidity range, where the masses were measured, was unclear. The masses of soils and fibers depend on their moisture content. Thus, the mass ratio should also depend on the humidity range.

3. Materials and Methods

3.1 Materials

Based on previous reports,^{16,19} mock-up materials simulating the upper- and middle-coat soils of the wall paintings were fabricated. Soil walls are sometimes used in traditional houses and cultural heritage buildings, and wall soil materials are commercially available. To prepare the specimens, wall soil for the middle coat was used. The soil was sorted according to particle size using the water-sieving method. Because the separation method between clay and fine sand in the literature¹⁶ was unclear, we regarded soil particles with a particle size of less than 75 μm , known as fine-grained soil in soil mechanics,³⁰ as *clay* referred to in the literature.¹⁶ To sort wall soils with different grain sizes, three types of industrial sieves were used, with mesh sizes of 2 mm, 500 μm , and 75 μm . Stacked sieves were placed on top of a pail, and the wall soil was added to the top sieve with water. The obtained gravel (larger than 2 mm), coarse and fine sands (500 μm –2 mm and 75–500 μm , respectively), and water containing clay (smaller

than 75 μm) were dried in an oven at 80°C. Figure 3A,B show the hemp and straw fibers used to fabricate the mock-up upper- and middle-coat soils, respectively. The width of the hemp fibers was less than 0.5 mm, and the length was approximately 10 mm for the most part, where the longest was 18 mm. The width of the straw fiber was in the range from less than 0.5 mm to approximately 4 mm, and the length was less than 40 mm. The length and diameter can affect the physical properties of the wall soils. However, the fibers added to the specimen were not sorted by their dimensions in this study. A further problem is clarifying the effects of fiber dimensions on the physical properties of the upper- and middle-coat soils.

Table 1 lists the materials and compositions of the soils. The fibers and separated soils were stored in a desiccator humidified to 53% relative humidity (RH). The mass compositions in Table 1 reflect the values at the same equilibrium RH. The materials and compositions of the mock-up wall soils were determined to be as similar as possible to those of the original wall painting substrate. However, one limitation is that they could not be proved to be the same as those of the original, and the difference could result in a misestimation of the mechanical properties. In addition, the effect of material composition on the material properties of wall soils could not be examined in this research, and additional confirmation that the measured mechanical properties are applicable to other artifacts with different material compositions is necessary.

Notably, the amount of water added to the upper-coat soil for strain measurement was larger to facilitate spreading with a trowel during specimen fabrication. Although no change in appearance was observed, the mechanical properties after drying could vary depending on the amount of water added during the specimen fabrication. Moreover, the *mizuawase* period was not considered in this study. *Mizuawase* changes the bridging

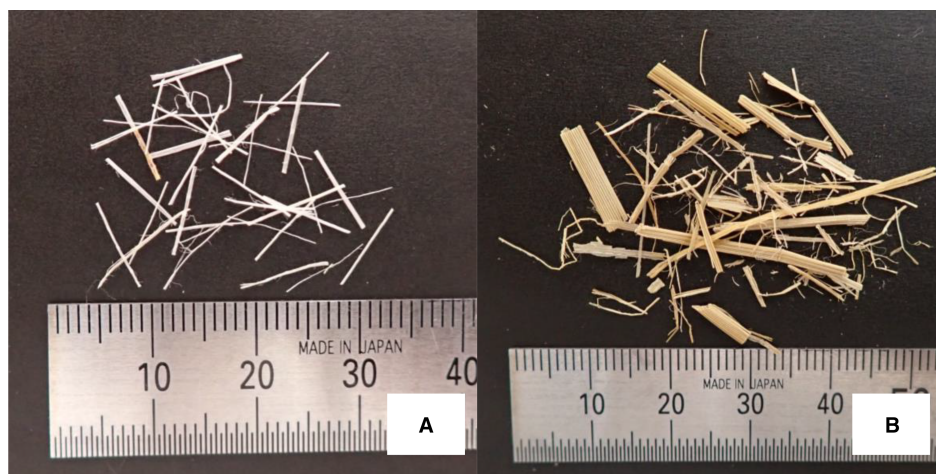


FIGURE 3 (A) Hemp and (B) straw fibers used to fabricate the mock-up wall soils

TABLE 1 Quantities of materials in the mock-up top-coat and middle-coat soils

Kind of soil	Fiber (g)	Clay (g) ~75 μm	Fine sand (g) 75–500 μm	Coarse sand (g) 500 μm –2 mm	Gravel (g) 2 mm ~	Water (g)
Upper-coat soil	0.11 (hemp)	14.13	84.01	1.87	–	25.18 (splitting tensile and compressive tests) 30.00 (strain measurement)
Middle-coat soil	3.54 (straw)	41.07	34.79	16.51	3.895	30.00

effect between clay and fibers and affects the viscosity of the wall soil paste. The physical properties, including the strength of the dried and hardened wall soil, are possibly affected by the *mizuawase*.^{20,21} Additionally, the chemical properties of wall soils, such as their elemental composition, ignition loss, the potential of hydrogen (pH), and electrical conductivity, have been investigated in previous research.²³ It has been reported that pH and electrical conductivity increased over the *mizuawase* period.³¹ The degree of the physical and chemical effects of *mizuawase* can depend on the length, temperature, types of soils, composition, and others.³¹ However, the conditions of *mizuawase* for the original substrate wall soils remains unclear, although it was possible that the properties of the wall soil were adjusted by *mizuawase* during the construction process of ancient buildings, including the main hall of Horyu-ji Temple. Simulating the change in properties of the wall soils due to *mizuawase* was difficult, and we fabricated the specimens without a *mizuawase* period, which was the most basic condition. The effects of *mizuawase*, which were not considered in this study, are required to be addressed in a future work.

Furthermore, as fundamental physical properties, Table 2 shows the dry density and porosity. To obtain the dry density, the dimensions were measured using a digital caliper. The composition of the upper-coat soil was the same as that used for the splitting tensile and compressive tests. The dry density was the average of three and six specimens for the upper- and middle-coat soils, respectively, oven-dried at 105°C. The porosity was measured using the mercury intrusion method using one specimen for each soil type. The range of the injection pressure was 7.377×10^{-3} to 4.086×10^2 MPa. The wall soils are fragile materials, and the specimens could be cracked microscopically during the mercury injection process, although visible cracks could not be found. The development of microscopic cracks potentially resulted in overestimating the porosity.

3.2 Test principles

Table 3 lists the test names, apparatuses, measurement targets, and materials used in this study. Three tests were performed: splitting tensile test, uniaxial compressive test, and humidity-induced strain measurement. The splitting tensile and

TABLE 2 Dry density and porosity of the upper- and middle-coat soils

Kind of soil	Dry density (kg/m ³)	Porosity (m ³ /m ³)
Upper-coat soil	1646	0.3192
Middle-coat soil	1487	0.3300

TABLE 3 Test name and corresponding test equipment, mechanical properties, and material

Test name	Test equipment	Mechanical properties	Material
Splitting tensile test Compressive test	Mechanical testing machine	Tensile strength	Upper-coat soil
	Mechanical testing machine	Compressive strength Young's modulus Proportional limit (Stress–strain relationship)	Upper-coat soil
Measurement of humidity-induced strain	Two-axis strain gauge	Poisson's ratio	Upper-coat soil
	Strain gauge	Moisture expansion coefficient	Upper-coat soil
	Data logger	(Humidity-induced strain)	Middle-coat soil

uniaxial compressive tests were performed only on the upper-coat soil specimens. Humidity-induced strain measurements were performed on the upper- and middle-coat soil specimens.

The principles for the splitting tensile and uniaxial compressive tests are described in the authors' previous study,² and we explain the outlines here. In the splitting tensile test, a compressive force was applied to the side of the cylindrical specimen, and a tensile force was applied perpendicular to the direction of the applied force. The maximum tensile stress σ_{max} (MPa) applied to the specimen can be obtained from the theoretical relationship between the specimen diameter D (m), specimen height L (m), and applied force P (MN)³²:

$$\sigma_{max} = \frac{2P}{\pi DL} \quad (7)$$

where the tensile strength is the tensile stress at break. In the uniaxial compressive test, an unconstrained cylindrical specimen was compressed in the axial direction. The stress–strain relationship was obtained from the displacement, applied force, and specimen dimensions. Young's modulus was obtained as the slope of the stress–strain relationship. To measure Poisson's ratio, the axial and circumferential strains were measured using a strain gauge attached to the side of the specimen. Notably, gauge glue can harden soft materials, including wall soils, making accurate measurements challenging. However, for simplicity, this study used strain gauges. The aim of measuring these mechanical properties was to contribute to the damage prediction of wall paintings. Therefore, we considered visible cracking to be “damage” in both tests, and regarded the stress at soil cracking as the strength, regardless of bearing capacity against the applied force.

In humidity-induced strain measurements, the specimen to which a strain gauge was attached was subjected to a constant degree of environmental humidity variation at a constant temperature. Material expansion or shrinkage corresponding to the change in RH was measured using a strain gauge. The relationship between the change in RH (drying and wetting from a reference RH value) and strain was obtained. Furthermore, the moisture expansion coefficient in response to changes in RH was estimated. Notably, similar to the Poisson's ratio measurement, the hardening of wall soils could occur, potentially resulting in an underestimation of the absolute value of strain.

3.3 Specimen preparation

Similar to a previous study,² metal water pipes were used as molds for the splitting tensile and compressive tests. The pipe lengths were 50 and 75 mm for the splitting tensile and compressive tests, respectively. The nominal diameter was 32 mm

for both tests. To prevent damage to the specimen during drying shrinkage, a rubber sheet was placed around the inner of each mold. The wet soil paste was poured into molds placed on sponge sheets. The specimens were naturally dried in a thermostatic chamber at 23°C. Although the humidity in the chamber was uncontrolled, it was monitored and ranged from 20% to 45% RH during specimen drying. The molds were removed 1 week after the paste was filled, and the specimens were dried in the same chamber for another 2 weeks. Subsequently, the bases of the specimens were smoothed using sandpaper. The heights of the specimens used for the splitting tensile and compressive tests were approximately 35 and 55 mm, respectively. Although attempts were made to fabricate upper- and middle-coat soil specimens, those for the middle-coat soil failed because the straw fiber in the soil obstructed the smoothing process. After the specimen preparation, the dimensions were measured using a digital caliper. Strain gauges were attached to the sides of the compressive test specimens. The specimens were then placed in desiccators humidity-conditioned with saturated salt. Four equilibrium humidity levels were selected: 105°C oven-dried (regarded as 0% RH), 33%, 53%, and 84% RH. Saturated salts were used to humidify the specimens. $MgCl_2 \cdot 6H_2O$ was for 33% RH, $Mg(NO_3)_2 \cdot 6H_2O$ for 53% RH, and KCl for 84% RH. The equilibrium humidity corresponding to each salt was referred from the literature.³³ The humidity conditioning periods of the specimens were at least 14 and 90 days for oven drying and the other humidity levels, respectively. Five specimens were tested for each splitting tensile and compressive test.

For humidity-induced strain measurements, specimens of 55 mm × 55 mm square with a 10-mm thickness were prepared using silicon molds for the upper- and middle-coat soil. The wet soil paste was plastered into the molds on a sponge sheet and allowed to dry naturally. Drying was conducted in an experimental room in winter, where temperature and humidity remained uncontrolled. The molds were removed 1 week after plastering the specimen paste. Six specimens were prepared for the upper-coat soil and five for the middle-coat soil.

The specimens used for the splitting tensile and compressive tests and those used for the humidity-induced strain measurements had different shapes and drying conditions. These differences could lead to differences in the measured material properties. Such changes in material properties related to the

preparation methods of the test specimens will be investigated in a future study.

3.4 Measuring system and methodology

The measuring apparatus and systems used for the splitting tensile and compressive tests were the same as those used in the authors' previous study.² Both tests were performed in a thermostatic chamber at 23°C. In both tests, humidity in the chamber remained uncontrolled for the 84% RH equilibrium specimens, with chamber humidity levels ranging from 71% to 86% RH. For the other RH equilibrium specimens, a domestic-sized dehumidifier was operated during the tests, maintaining humidity levels of approximately 60%–72% RH for the 53% RH equilibrium specimens and approximately 44%–53% RH for the 33% RH equilibrium and oven-dried specimens. For cooling, the oven-dried specimens were moved into a desiccator dried with silica gel in the thermostatic chamber at 23°C approximately 1 h before the tests. The loading ratios of the splitting tensile and compressive tests were determined according to JGS 2551-2020 and JGS 2521-2020,³² set at 0.1 mm/min and 0.05 mm/min, respectively. In the splitting tensile test, loading was stopped at least 10 min after commencement and when a crack was visually observed on the base. In the compressive test, loading was stopped for at least 20 min and when a crack was observed on the side.

Figure 4 shows the measuring system for the humidity-induced strain measurements. The strain measurement system comprised an NR-600 logger and NR-ST04 (Keyence Co.) (Figure 4A). Strain gauges and gauge glue were KFGS-30-120-C1-11 and CC-35 (Kyowa Electronic Instruments Co., Ltd.) (Figure 4B), respectively. The measurements were conducted in a thermostatic room at 23°C. Each specimen was placed on a glass dish in a humidity-conditioned desiccator with a saturated salt solution at the reference relative humidity. The strain at equilibrium was set to zero. The salt solution was replaced to dry/humidify the desiccator, and the strains of the specimens caused by a difference in RH between the reference and new relative humidities were recorded. The reference humidity was 53% RH, and the humidities under drying and humidifying conditions were 33% and 84%, respectively. Owing to the limited logger-connection capacity, the specimens were divided into two groups (A and B) and placed in different desiccators. Each group contained three specimens of

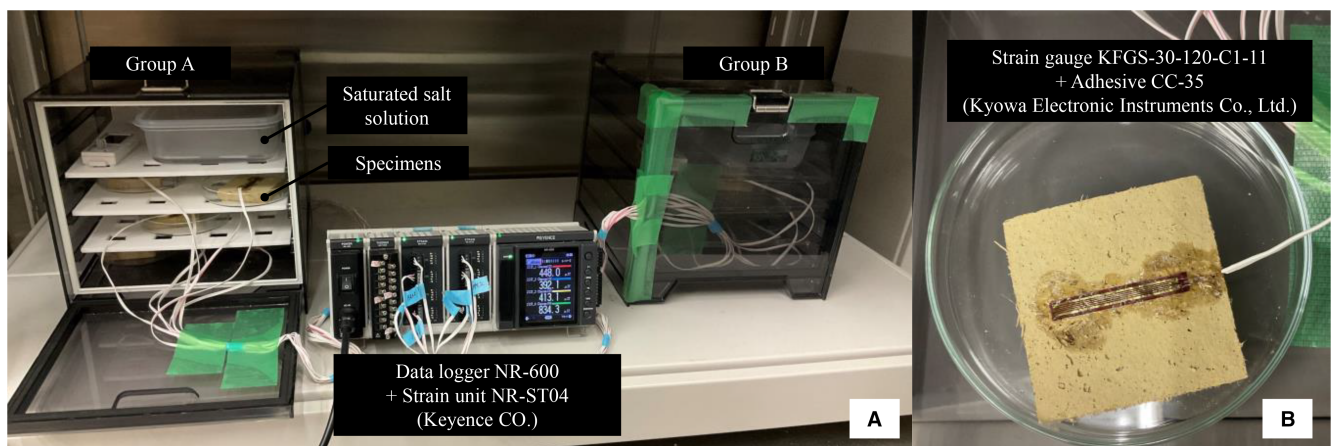


FIGURE 4 Measuring equipment of humidity-induced strain

the upper-coat soil and two to three specimens of the middle-coat soil.

4. Results

4.1 Tensile strength

Figure 5 shows the relationship between the test force and ratio of the displacement to the specimen diameter during the splitting tensile test at each equilibrium humidity. As a typical example of the failure process, the appearance of a specimen base (red line) during the test is shown in Figure 5. The test force linearly increased with the displacement-to-diameter ratio at every equilibrium RH, reaching a local maximum value before the ratio reached 0.02. It is considered that the initial increase in the slope was attributed to the increasing surface area supporting the applied force with increasing displacement when the side surface of the specimen was rough. For most specimens, the test force decreased immediately after reaching the local maximum value. Subsequently, the test force tended to increase until the end of the test for all specimens, although the base had already cracked. We expect that the first maximum value was attributed to the bonding of the soil and sand, and the subsequent increase in the test force was attributed to the support provided by the hemp fiber against tensile force. As discussed in the Introduction, the occurrence of cracks in cultural artifacts leads to a loss in value, despite their capability to withstand tensile forces. Therefore, the tensile strength was obtained from the local maximum value of the test force (blue circle in Figure 5; red line).

Figure 6 shows the measured and average tensile strengths relative to the equilibrium RH. The average tensile strength

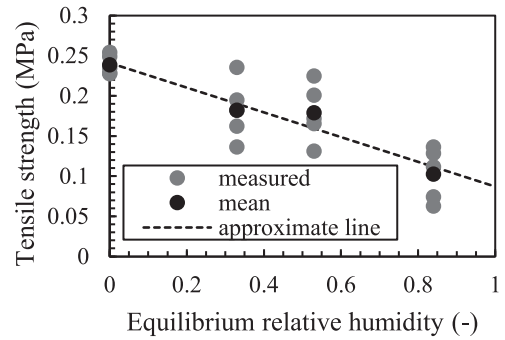


FIGURE 6 Relationship between the tensile strength of the upper-coat soil and equilibrium RH

ranged from 0.103 MPa to 0.239 MPa. The average tensile strength decreased with increasing equilibrium RH over the entire measured humidity range. We consider the relationship between tensile strength and relative humidity is not necessarily linear because it depends on the meniscus formation in the upper-coat soil. Notably, the measured tensile strengths of specimens at 33% and 53% equilibrium RH had similar ranges, and the average tensile strengths were not significantly different. However, the test results were insufficient to approximate a suitable curve and coefficients reflecting the relationship between mechanical properties, including tensile strength and relative humidity, owing to the limited humidity range used in the tests. Thus, the tensile strength σ_{ten} (MPa) was approximated as a linearly decreasing function of equilibrium RH h (-), expressed as follows:

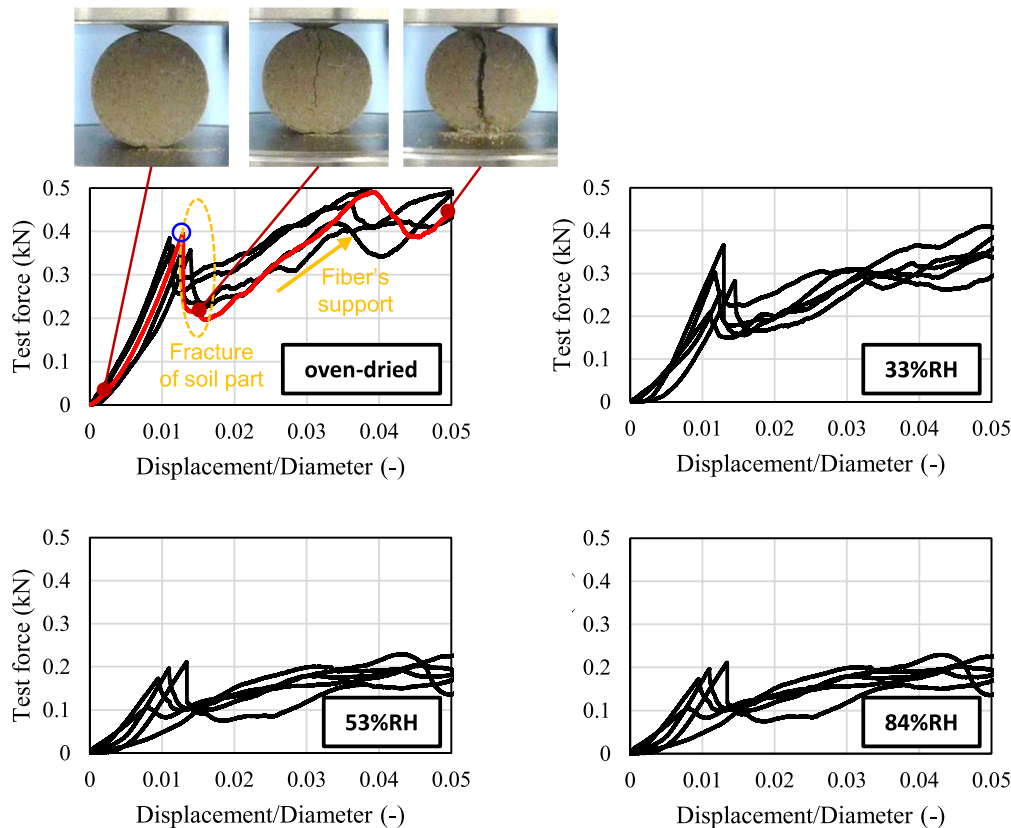


FIGURE 5 Test force–displacement/diameter relationship of the upper-coat soil during the splitting tensile test

$$\sigma_{ten} = -0.1539h + 0.2410. \tag{8}$$

The coefficients in Equation (8) were obtained using the least-squares method for four average values. The coefficient of determination was 0.944. To obtain a more detailed approximation, further studies on the relationship between tensile strength and humidity are necessary through tests with a finer humidity range. This requirement also applies to the mechanical properties, as discussed below.

4.2 Compressive strength

Figure 7 shows the stress–strain relationship observed during the compressive test for each equilibrium RH. As an example of the failure process, the change in the appearance of a specimen is shown in red line. For every equilibrium RH, the slope of the stress–strain curve initially increased within the range of 0.0–0.3 kPa. In the compressive test, it was considered that the initial increase in the slope was larger when the base of the specimen was a rough plane, with the rough part subsequently flattened by the compressive force. After the initial slope increase, the stress relative to the strain increased linearly. The maximum stress was reached after the slope decreased. Subsequently, the stress rapidly decreased. Similar to the red-line specimen, for every compressive test, side cracks were visually observed on the specimen after the stress decreased. Therefore, the compressive strength (blue solid circle in Figure 7) was determined as the maximum stress of the entire stress–strain relationship. Because the stress–strain relationship deviates from linearity before reaching the maximum stress, a proportional limit was also determined as the maximum stress to which Young’s modulus can

be applied. The Young’s modulus and proportional limit are defined in the subsequent section.

Figure 8 shows the measured and average compressive strengths relative to the equilibrium RH. The average compressive strength ranged from 1.16 MPa to 2.55 MPa. The compressive strength at the same humidity was 9.30–11.3 times greater than the tensile strength, confirming that upper-coat soil was weaker in tension. The average compressive strength decreased with increasing equilibrium RH. The relationship between the mechanical properties and equilibrium humidity is not necessarily linear when the meniscus formation influences the mechanical properties. However, in contrast to tensile strength, a clear linear relationship between compressive strength and equilibrium humidity was observed. The compressive strength σ_{com} (MPa) is expressed

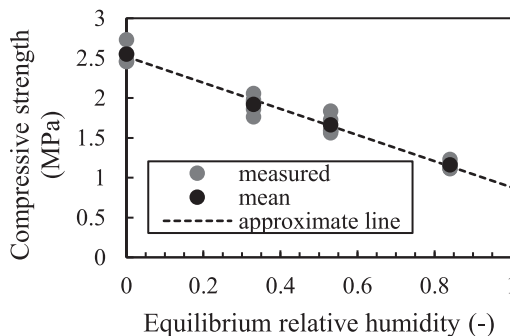


FIGURE 8 Relationship between the compressive strength of the upper-coat soil and equilibrium RH

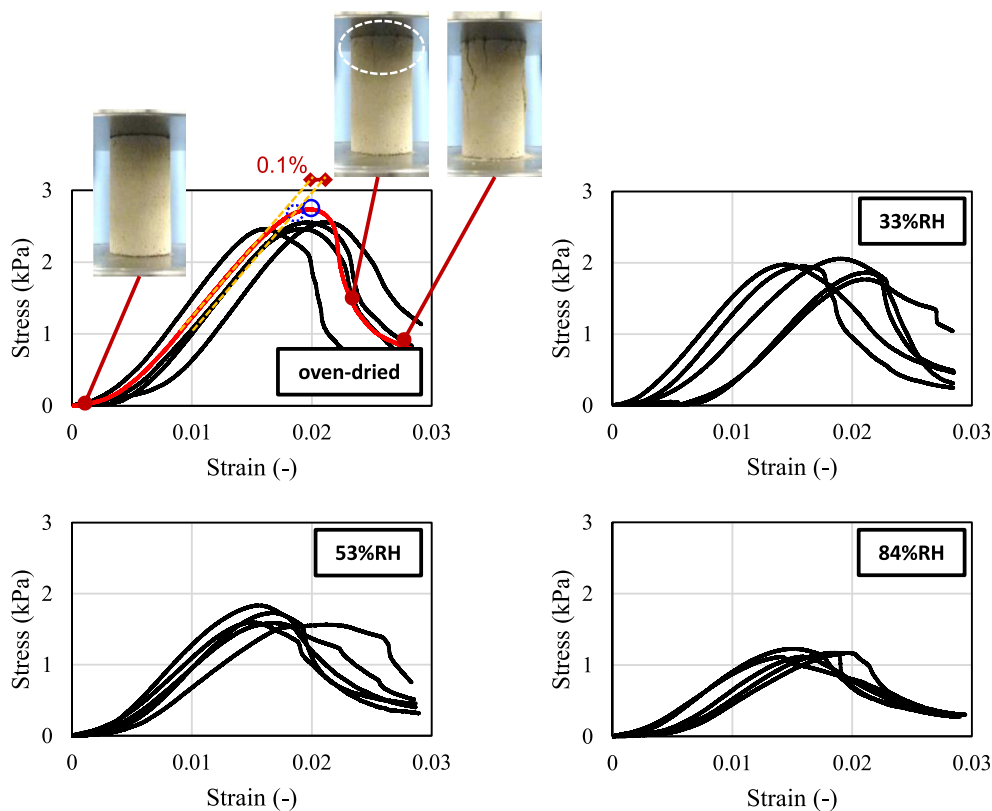


FIGURE 7 Stress–strain relationship of the upper-coat soil during the compressive test

as a linearly decreasing function of equilibrium RH h (–), as follows:

$$\sigma_{com} = -1.638h + 2.520. \quad (9)$$

The coefficients were obtained using the least-squares method, yielding a coefficient of determination of 0.995.

4.3 Young's modulus, proportional limit, and Poisson's ratio

Young's modulus was obtained from the slope of the stress–strain relation shown in Figure 7. The stress ranges where Young's modulus was obtained were 1.0–2.0 kPa for specimens oven-dried at 105°C, 0.7–1.2 kPa for 33% RH and 53% RH, and 0.3–0.8 kPa for 84% RH. In addition, the stress at which the corresponding strain deviated by 0.1% from the linear relationship of the slope of Young's modulus was determined as a proportional limit (blue dotted circle in Figure 7). Figures 9 and 10 show the measured and average Young's moduli and proportional limit relative to the equilibrium RH, respectively. The average Young's modulus and proportional limit ranged from 0.115 GPa to 0.209 GPa and 1.10 MPa to 2.49 MPa, respectively. Both values decreased with increasing equilibrium RH. Young's modulus E (GPa) and proportional limit σ_{pro} (MPa) were approximated as decreasing linear functions of equilibrium RH h (–), respectively.

$$E = -0.1129h + 0.2153 \quad (10)$$

$$\sigma_{pro} = -1.633h + 2.449 \quad (11)$$

The coefficients were obtained using the least-squares method, yielding coefficients of determination of 0.968 and 0.992, respectively.

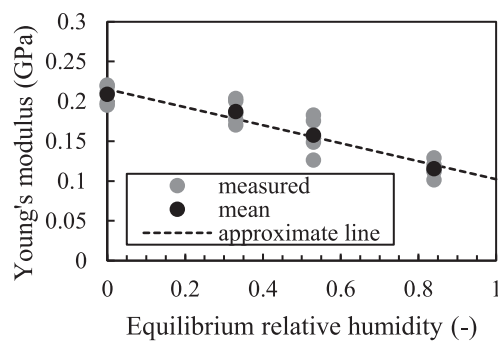


FIGURE 9 Relationship between Young's modulus of the upper-coat soil and equilibrium RH

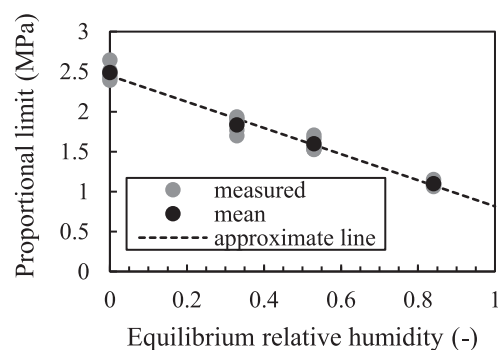


FIGURE 10 Relationship between the proportional limit of the upper-coat soil and equilibrium RH

Figure 11 shows the measured and average Poisson's ratios relative to the equilibrium RH. The average Poisson's ratios at each equilibrium RH were approximately 0.162, 0.147, and 0.146 (–) for 33, 53, and 84% RH, respectively. The average of the three values was 0.152 (–), and the mean absolute error was 0.018 (–) when the average value was regarded as the approximate Poisson's ratio.

4.4 Moisture expansion coefficient

Figure 12 shows the strain in each measurement group during drying and wetting. For all specimens, the strain increased during wetting and decreased during drying, and the change over time became smaller and nearly constant. Figure 13A,B show the time-averaged strain values during 500–550 h for dry and wet conditions for the upper- and middle-coat soils, respectively. The time-averaged strains of the upper- and middle-coat soils were approximately 372.3–434.8 μ ST and 738.6–869.3 μ ST at 84% RH and –238.9 to –199.2 μ ST and –390.3 to –347.7 μ ST at 33% RH, respectively. For each soil, the relationship between strain ϵ (μ ST) and equilibrium humidity (–) was expressed as a linear function, with the strain at 53% RH was 0 μ ST.

$$\epsilon_{humi} = e(h-0.53) \quad (12)$$

The moisture expansion coefficients were obtained using the least-squares method, and the values for the upper- and middle-coat soils are listed in Table 4. The coefficients of determination were 0.995 and 0.980, respectively. The moisture expansion coefficient of the middle-coat soil was nearly twice that of the upper-coat soil. Further study on the effects of the types of materials and wall soil composition on the expansion properties would be valuable.

5. Discussions

The measurements clarified the strength and elastic moduli of the upper-coat soil simulating the substrate of *Hiten* wall paintings in the main hall of Horyu-ji Temple. To confirm the validity of the mechanical properties of the upper-coat soil, the results in this study were compared with those from previous research.^{20–27} The mechanical properties of wall soil depend on the material, composition, fabrication methods, and other factors, such as the measurement method. Therefore, a simple comparison of test results is difficult. With this caution in mind, compressive and tensile strengths and elastic modulus of wall soils are shown in Table 5. These mechanical properties

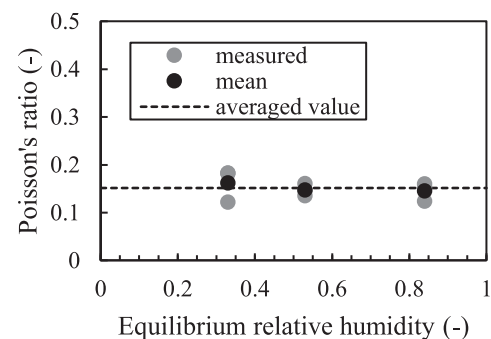


FIGURE 11 Relationship between Poisson's ratio of the upper-coat soil and equilibrium RH

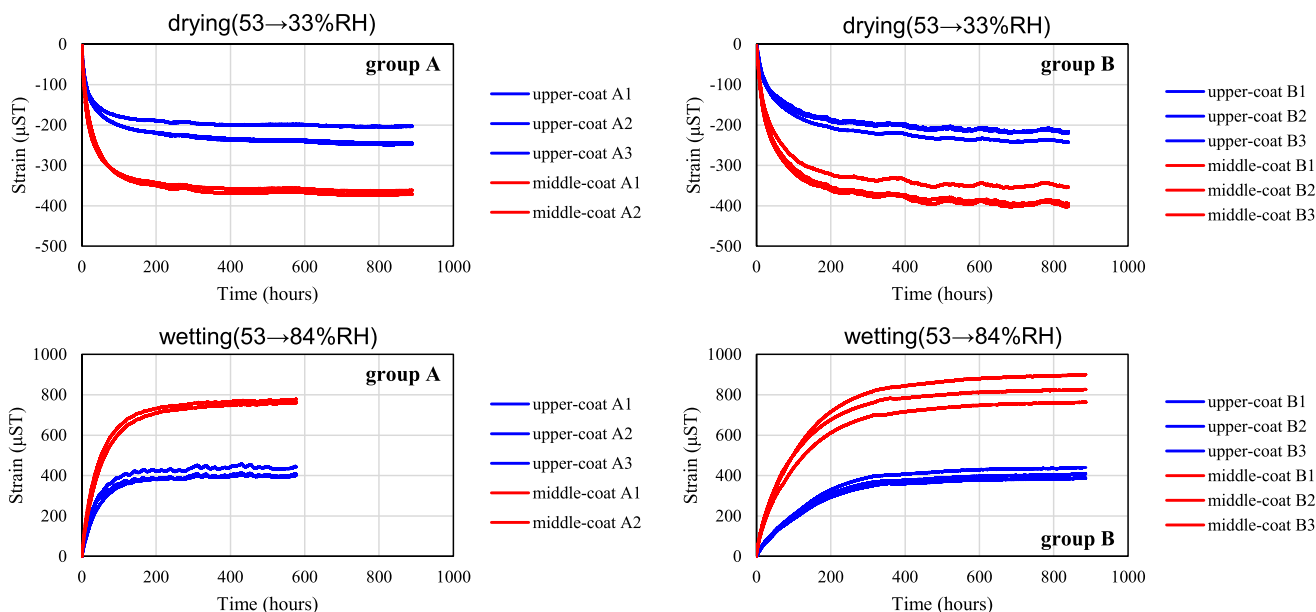


FIGURE 12 Strain decreasing/increasing over time

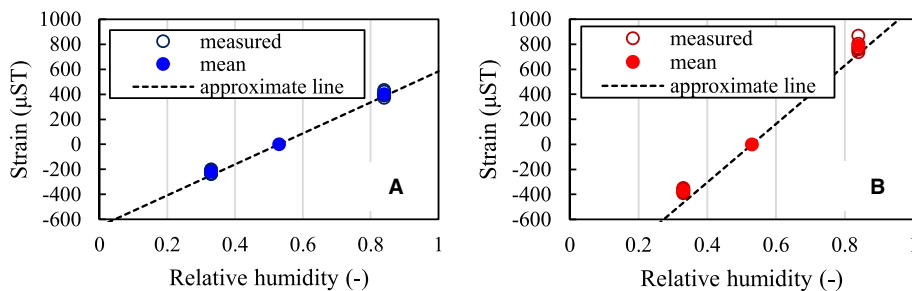


FIGURE 13 Humidity-induced strains of the upper- and middle-coat soils

TABLE 4 Moisture expansion coefficients of the upper- and middle-coat soils

Material	Value of expansion coefficient ϵ ($\mu\text{ST}/\text{--}$)
Upper-coat soil	1240
Middle-coat soil	2337

were referenced from studies targeting Japanese wall soils, including under-, middle-, and sub-middle-coat soils, because the material, composition, and fabrication methods were considered similar to the upper-coat soil in this study. *Nakatsuketuchi* in literature²² was translated into sub-middle-coat soil, representing the layer between the under- and middle-coat soils. The variable factors used in the previous studies were presented in the “variable” column. Consequently, the compressive strength of the upper-coat soil was within the range reported in the literature. Young’s modulus of the upper-coat soil was slightly lower than the elastic modulus in previous research. The tensile strength was measured using different methods (direct tensile test^{22,25} and splitting tensile test²⁴); however, that of the upper-coat soil was almost within the range of the previous research results. Poisson’s ratio of the upper-coat soil was evaluated in this study and had little

dependency on the equilibrium humidity. However, no referenceable value was available for Poisson’s ratio, although several studies have conducted uniaxial compressive tests. This can be attributed to the difficulty in attaching strain gauges to wall soil specimens and the hardening of the specimens caused by gauge glue, making the measurement of Poisson’s ratio challenging. Noncontact displacement measurement methods, such as x-ray computed tomography, will enable measurements that are not affected by the hardening caused by gauge glue, offering a possible solution. In addition, in previous studies, the failure process of the wall soil was assumed to be brittle, and a proportional limit was not indicated. The proportional limit of the upper-coat soil was 95–98% of the compressive strength in this study. Thus, in damage prediction of wall paintings, the proportional limit of the compression-side limit enables a simple but slightly risky side calculation. In this study, the compressive strength and proportional limit were indicated separately for clarity and precision.

The tensile and compressive strengths, Young’s modulus, and proportional limit of the upper-coat soil decreased with increasing equilibrium RH, similar to the white clay in the authors’ previous study.² Hirano et al.²¹ also performed compressive tests on under-coat soil specimens at different equilibrium RH values (with different *mizuawase* periods), indicating

TABLE 5 Mechanical properties of wall soils indicated in the existing literature

Reference	Kind of wall soil	Mechanical properties	Unit	Value	Variable
Ura et al. ²⁰	Under coat	Compressive strength	MPa	0.3–0.7 ^a	Sample shape
			MPa	1.1 ^a	Compactness
			MPa	0.5–0.8 ^a	Length of <i>mizuawase</i> period
			MPa	1.3 ^a	Temperature, humidity during curing
Hirano et al. ²¹	Under coat	Compressive strength	MPa	0.3–4.5 ^a	Length of <i>mizuawase</i> period, Composition of fiber, Equilibrium humidity
Nakao et al. ²²	Under coat	Compressive strength	MPa	0.20–0.42 ^a	–
		Tensile strength	MPa	0.02–0.07 ^a	
	Middle coat	Compressive strength	MPa	0.39–0.66 ^a	
		Tensile strength	MPa	0.02–0.15 ^a	
	Sub-middle coat	Compressive strength	MPa	0.51–0.64 ^a	
		Tensile strength	MPa	0.08–0.15 ^a	
Koshiishi and Inden ²³	Under coat	Compressive strength	MPa	1.76–3.43	Dry density, soil production area, mixing materials
	Middle coat	Compressive strength	MPa	1.09–1.98	Dry density, soil production area
Nakao and Yamazaki ²⁴	Middle coat (without sand and fiber)	Compressive strength	MPa	Average: 1.11 Range: 0.45–1.79	Soil production area
		Tensile strength	MPa	Average: 0.12 Range: 0.04–0.23	
	Middle coat (with sand and fiber)	Compressive strength	MPa	0.97–1.47 ^a	
		Tensile strength	MPa	0.10–0.17 ^a	
Ura and Yamamoto ²⁵	Under coat	Compressive strength	MPa	0.25–1.25 ^a	Composition of clay and sand, soil production area
		Tensile strength	MPa	0.1–0.2 ^a	
Yamada and Koshiishi ²⁶	Under coat	Elastic modulus	GPa	0.2–1.2	Fiber content, soil production area, grain size
		Compressive strength	MPa	0.3–2.3 ^a	Dry density, soil production area, grain size
	Middle coat	Elastic modulus	GPa	0.4–1.1 ^a	Fiber content, grain size
		Compressive strength	MPa	0.3–1.7 ^a	Dry density, grain size
Ochi et al. ²⁷	Middle coat	Elastic modulus	GPa	0.17–0.28	Soil production area
		Compressive strength	MPa	0.52–0.98	

^a Value read from figures in the literature.

a trend similar to that of the upper-coat soil in this study. As mentioned in a previous study,² the microscopic bond caused by the meniscus between the soil particles will be responsible for the strength and elasticity measured macroscopically. The intensity of the bond depends on the capillary pressure, surface tension of the liquid water, and the geometry of the meniscus.³⁴ Among these factors, capillary pressure decreases with increasing equilibrium RH. This could be responsible for diminishing the bond between soil particles, leading to macroscopically decreasing tensile and compressive strengths and Young's modulus. Furthermore, the range of equilibrium RH in the tensile splitting and compressive tests ranged from oven drying to 84% RH, and the approximate lines were obtained to fit the results within the humidity range. However, it can be inferred that soil can lose its structure in high-humidity environments near 100% RH because the space between soil particles is filled with liquid water, diminishing meniscus formation. Therefore, the tensile and compressive strengths and Young's modulus can significantly decrease in the high-humidity range, which was not measured in this study.

On the other hand, no previous studies have measured the moisture expansion coefficients of the upper- and middle-coat soils after drying and being hardened. The measured humidity-induced strain can contribute to damage prediction in the targeted wall paintings and crack-occurrence prediction in clay-based cultural artifacts and soil walls in traditional

Japanese houses. It is noteworthy that the moisture expansion coefficients of the upper- and middle-coat soils were approximated from the measured strain at drying (53%–33% RH) and wetting (53%–84% RH) and did not cover extremely dry or over-hygroscopic ranges. When strain gauges are attached to soft materials such as wall soils, the gauge glue can harden the surface of the material around the gauge and make the materials difficult to deform. In our study, the measured value was the amount of deformation of the glue-hardened surface, and the deformation was potentially smaller than that measured by other methods, under which the gauge glue does not have an effect. Optical strain measuring methods, including the digital image correlation method, should be used in future studies.

6. Conclusions

This study measured the mechanical properties of upper- and middle-coat soils using mock-up materials simulating the substrate of *Hiten* wall paintings in the main hall of Horyu-ji Temple. For the upper-coat soil, Young's modulus, Poisson's ratio, the proportional limit, and compressive strength were determined through uniaxial compressive test, and the tensile strength through tensile splitting test. The upper-coat soil comprised dried soil, water, and hemp fibers and its structure is supported by meniscus between the soil particles. Therefore, the mechanical properties of the upper-coat soil were expected

to be significantly dependent on equilibrium humidity. The humidity dependence of elastic coefficients and strengths was quantified using specimens at various equilibrium RH values. The tensile strength, compressive strength, Young's modulus, and proportional limit of the upper-coat soil were approximately 0.103–0.239 MPa, 1.16–2.55 MPa, 0.115–0.209 GPa, and 1.10–2.49 MPa, respectively, in the humidity range of oven drying (105°C) to 84% RH. The tensile and compressive strengths, proportional limits, and Young's moduli decreased with increasing equilibrium RH. Poisson's ratio was approximately 0.152 (–), regardless of the equilibrium RH. The humidity-induced strains of the upper- and middle-coat soils were measured, and the strain–equilibrium RH relationships of both soils were clarified. The moisture expansion coefficients of the upper- and middle-coat soils were approximately 1240 and 2337 ($\mu\text{ST}/\text{--}$), respectively.

The mechanical properties of the upper-coat soil and the moisture expansion coefficients of the upper- and middle-coat soils can be used for damage prediction in *Hiten* wall paintings. The results can also be beneficial for the conservation or repair projects of cultural artifacts in which wall soil is used. However, the applicability of the results of this study should be confirmed because the mechanical properties of earth materials depend on the mixing materials, composition, and measuring methods. Furthermore, the results of this study can facilitate a better understanding of the effects of moisture conditions on the mechanical properties and dimensional changes in wall soils. Future research should explore other mechanical and hygrothermal properties of the materials used in *Hiten* wall paintings for damage prediction of the wall paintings. Moreover, a numerical simulation model is necessary to clarify the environmental conditions required for their safe and effective conservation.

Acknowledgments

We would like to appreciate the cooperation to the persons of Horyu-ji temple, The Ashahi Shinbun Company and Agency for Cultural Affairs (Government of Japan), who are part of the office of the committee for the conserving and utilizing of the wall paintings at Kondo in Horyu-ji temple. We are also gratefully appreciative of the opportunity to engage in insightful discussions about the composition of the wall paintings with Dr. Norimasa Aoyagi, Associate Professor at Ritsumeikan University. We would further like to appreciate indispensable cooperation in creating the test specimens of Mr. Yasushi Toyoda and Mr. Takeo Toyoda, representatives of Toyoda Yasushi architectural designing office and Toyoda plastering work company (Toyoda Kogyo-sho). Finally, we would like to thank Editage (www.editage.jp) for English language editing.

Disclosures

The authors have no conflict of interest.

Data availability statement

The data that support the findings of this study are available from the corresponding author upon reasonable request.

References

- Harriman L, Brundrett G, Kittler R. *Humidity Control Design Guide for Commercial and Institutional Buildings*. American Society of Heating, Refrigerating and Air-Conditioning Engineers; 2001.
- Ishikawa K, Ogura D, Iba C, Takatori N, Wakiya S. Mechanical properties of white clay used in wall paintings: measurement of strength and modulus of elasticity of simulated substrate material of paintings *Hiten* at Kondo, the main hall at Horyu-ji Temple. *Herit Sci*. 2023;11:242.
- Matsumoto M, Iwamae A. An analysis of temperature and moisture variations in the ground under natural climatic conditions. *Energ Buildings*. 1988;11:221–237.
- Mecklenburg MF, Tumosa CS. Mechanical Behavior of Paintings Subjected to Changes in Temperature and Relative Humidity. In: Mecklenburg MF, ed. *Art in Transit: Studies in the Transport of Paintings*. National Gallery of Art; 1991:173–216.
- Mecklenburg MF, Tumosa CS, Erhardt D. Structural Response of Painted Wood Surfaces to Changes in Ambient Relative Humidity. In: Dorge V, Howlett FC, eds. *Painted Wood: History and Conservation*. The Getty Conservation Institute; 1998:464–483.
- Mazzanti P, Togni M, Uzielli L. Drying shrinkage and mechanical properties of poplar wood (*Populus alba* L.) across the grain. *J Cult Herit*. 2012;13S: S85–S89.
- Jakiela S, Bratasz L, Kozłowski R. Numerical modelling of moisture movement and related stress field in lime wood subjected to changing climate conditions. *Wood Sci Technol*. 2008;42:21–37.
- Rachwał B, Bratasz L, Łukomski M, Kozłowski R. Response of wood supports in panel paintings subjected to changing climate conditions. *Strain*. 2012;48:366–374.
- Janas A, Fuster-López L, Andersen CK, et al. Mechanical properties and moisture-related dimensional change of canvas paintings—canvas and glue sizing. *Herit Sci*. 2022;10:160.
- Rachwał B, Bratasz L, Krzemiński L, Łukomski M, Kozłowski R. Fatigue damage of the gesso layer in panel paintings subjected to changing climate conditions. *Strain*. 2012;48:474–481.
- Bratasz L, Akoglu KG, Kélicheff P. Fracture saturation in paintings makes them less vulnerable to environmental variations in museums. *Herit Sci*. 2020;8:11.
- Janas A, Mecklenburg MF, Fuster-López L, et al. Shrinkage and mechanical properties of drying oil paints. *Herit Sci*. 2022;10:181.
- Bridarolli A, Freeman AA, Fujisawa N, Łukomski M. Mechanical properties of mammalian and fish glues over range of temperature and humidity. *J Cult Herit*. 2022;53:226–235.
- Luimes RA, Suiker ASJ, Verhoosel CV, Jorissen AJM, Schellen HL. Fracture behaviour of historic and new oak wood. *Wood Sci Technol*. 2018;52:1243–1269.
- Schellmann NC, Taylor AC. Establishing the fracture properties of delaminating multilayered decorative coatings on wood and their changes after consolidation with polymer formulations. *J Mater Sci*. 2015;50:2666–2681.
- Fujii K. *Integration of the Report on the Repair Work for Buildings of National Treasures and Important Cultural Properties (4th Supplementation), Report on the Repair Work for Conservation of National Treasures in Horyu-ji Temple*. Vol 14. Bunsei shoin; 1956 (in Japanese).
- Committee to investigate methods of conservating the wall paintings of Horyu-ji temple. Report on a Survey of Conservation Methods for Wall Paintings of Horyu-ji Temple. 1920. (in Japanese). <https://dl.ndl.go.jp/pid/957032/1/1>. Accessed March 31, 2023.
- Yamada S. Report on Ancient Wall Paintings. 1975. (in Japanese).
- Aoyagi N, Hayashi H. Structural Details of Ancient Wall in the First Story of the Horyuji Main Hall Built in 7th Century. In proceedings of the annual research meeting of Architectural Institute of Japan (AIJ) Kinki Chapter. No. 9002, pp. 361–364. (in Japanese).
- Ura N, Gamada S, Suzuki Y. Fundamental experiment on test-piece preparation and strength test method of the kabetsuchi. *J Struct Constr Eng, AIJ*. 2002;67(559):23–30. (in Japanese).
- Hirano Y, Arima T, Shida S. Effect of seasoning time for wall clay with water and straw on material characteristic. *J Jpn Soc Finish Tech*. 2003;10(1):1–7. (in Japanese).
- Nakao M, Ichimonji R, Yamazaki Y, Ishibashi Y. An experimental study on shear resisting mechanism and shear strength evaluation method of mud-plastered walls. *J Struct Constr Eng, AIJ*. 2005;70(589):109–116. (in Japanese).
- Koshiishi N, Inden T. Properties of wall clays in main districts – wall clays for clay wall on bamboo lathing part 1. *J Struct Constr Eng, AIJ*. 2008;73(631):1467–1474. (in Japanese).
- Nakao M, Yamazaki Y. Estimation of range of maximum shear stress on mud-plastered wall based on material testing of mud. *J Struct Constr Eng, AIJ*. 2010;75(649):601–607. (in Japanese).
- Ura N, Yamamoto T. Property of the original soil for wall clay of a region. *AIJ J Technol Des*. 2011;17(36):449–454. (in Japanese).
- Yamada M, Koshiishi N. Properties of wall clays with straws – wall clays for clay wall on bamboo lathing part 2. *J Struct Constr Eng, AIJ*. 2013;78(689):1209–1218. (in Japanese).
- Ochi T, Miyamoto M, Utsunomiya N, Kobayashi M, Yamanaka M, Matsushima M. Effect of mix proportion on deformation and strength characteristics of wall clay. *AIJ J Technol Des*. 2015;21(48):461–465. (in Japanese).
- Nakao M, Yamazaki Y, Tanaka J. An experimental study on evaluating shear strength of mud-plastered walls. *J Struct Eng*. 2003;49:573–578. (in Japanese).

- 29 Miyoshi K, Hayasaki Y, Syojo N, Ohashi Y. Proposal of strength estimation formula of wall clays using multiple regression analysis – a study on the strength of mud walls (part 1). *J Struct Constr Eng, AIJ*. 2019;**84**(761):937-947. (in Japanese).
- 30 Terzaghi K, Peck RB, Mesri G. *Soil Mechanics in Engineering Practice*. Third ed. John Wiley and Sons; 1996.
- 31 Yamada M, Koshiishi N, Inden T. Fundamental study on properties of clays for mud walls: Report 7 Influence of MIZUAWASE on properties of wall clay and chopped straw. In summaries of technical papers of Architectural Institute of Japan (AIJ) annual meeting (Kyushu). No. 1319, pp. 653–654. 2007. (in Japanese).
- 32 Japanese geotechnical society. *Japanese Standards and Explanations of Laboratory Tests of Geomaterials (the First Revised Edition)*. Maruzen; 2020. (in Japanese).
- 33 Architectural Institute of Japan Environmental Standards. *Standard for Measurement of Moisture Properties AIJES-H0001-2020*. Maruzen; 2020. (in Japanese).
- 34 Butt H, Graf K, Kappl M. *Physics and Chemistry of Interfaces. Third, Revised and Enlarged Edition*. Wiley; 2013.

How to cite this article: Ishikawa K, Ogura D, Iba C, Takatori N, Wakiya S. Mechanical properties of wall soils for predicting damage to the substrate of *Hiten* wall paintings in the Horyu-ji Temple main hall caused by humidity fluctuation: Measurements with mock-up materials. *Jpn Archit Rev*. 2024;**7**:e70000. <https://doi.org/10.1002/2475-8876.70000>